The polyphased tectonic evolution of the Anegada Passage in the northern Lesser Antilles subduction zone

Muriel Laurencin, Boris Marcaillou, D. Graindorge, F. Klingelhoefer, Serge Lallemand, M. Laigle, Jean-Frederic Lebrun

AGU PUBLICATIONS

Tectonics

RESEARCH ARTICLE
10.1002/2017TC004511

Key Points:
- New bathymetric and seismic data highlight the deformation pattern of the northern Lesser Antilles active margin
- The Anegada Passage is a NE-SW trending past structure which is opened by NW-SE extension due to the collision of the Bahamas Bank
- Strain partitioning, related to the plate convergence obliquity, currently deforms the Anegada Passage by a WNW-ESE shear strain.

Correspondence to:
M. Laurencin,
muriel.laurencin@univ-brest.fr

Citation:
Laurencin, M., B. Marcaillou, D. Graindorge, F. Klingelhoefer, S. Lallemand, M. Laigle, and J.-F. Lebrun (2017), The polyphased tectonic evolution of the Anegada Passage in the northern Lesser Antilles subduction zone, *Tectonics*, *36*, 945–961, doi:10.1002/2017TC004511.

Received 9 FEB 2017
Accepted 3 MAY 2017
Accepted article online 6 MAY 2017
Published online 24 MAY 2017

The polyphased tectonic evolution of the Anegada Passage in the northern Lesser Antilles subduction zone

M. Laurencin[1], B. Marcaillou[2], D. Graindorge[1], F. Klingelhoefer[3], S. Lallemand[4], M. Laigle[2], and J.-F. Lebrun[5]

[1]Geosciences Océan, UMR 6538, Université Bretagne Occidentale / Institut Universitaire Européen de la Mer, Place N. Copernic, Plouzané, France, [2]Université Côte d'Azur, CNRS, Observatoire de la Côte d'Azur, IRD, Géoazur, Valbonne, France, [3]Ifremer, Brest, France, [4]Geosciences Montpellier, Université de Montpellier, Montpellier, France, [5]Géosciences Montpellier, Université des Antilles, Pointe à Pitre, France

Abstract The influence of the highly oblique plate convergence at the northern Lesser Antilles onto the margin strain partitioning and deformation pattern, although frequently invoked, has never been clearly imaged. The Anegada Passage is a set of basins and deep valleys, regularly related to the southern boundary of the Puerto Rico-Virgin Islands (PRVI) microplate. Despite the publications of various tectonic models mostly based on bathymetric data, the tectonic origin and deformation of this Passage remains unconstrained in the absence of deep structure imaging. During cruises Antithesis 1 and 3 (2013–2016), we recorded the first deep multichannel seismic images and new multibeam data in the northern Lesser Antilles margin segment in order to shed a new light on the structure and tectonic pattern of the Anegada Passage. We image the northeastern extent of the Anegada Passage, from the Sombrero Basin to the Lesser Antilles margin front. Our results reveal that this northeastern segment is an EW trending left-stepping en échelon strike-slip system that consists of the Sombrero and Malliwana pull-apart basins, the Malliwana and Anguilla left-lateral faults, and the NE-SW compressional restraining bend at the Malliwana Hill. Reviewing the structure of the Anegada Passage, from the south of Puerto Rico to the Lesser Antilles margin front, reveals a polyphased tectonic history. The Anegada Passage is formed by a NW-SE extension, possibly related to the rotation or escape of PRVI block due to collision of the Bahamas Bank. Currently, it is deformed by an active WNW-ESE strike-slip deformation associated to the shear component of the strain partitioning resulting from the subduction obliquity.

1. Introduction

The Anegada Passage is a deep NE-SW trending trough that includes a set of faults and basins from the Whiting Basin up to the Southwest to the Sombrero Basin to the northeast (Figure 1). This passage is located across the volcanic arc at the transition between the Greater and the Lesser Antilles islands where the subduction front reaches its maximum curvature. Numerous studies document this deep and elongated bathymetric structure to the southeastern limit of the Puerto Rico Virgin Island (PRVI) microplate [e.g., *Jany et al.*, 1990] which reveal the Anegada Passage great influence onto the geodynamic and the kinematic evolution of the area. These studies mainly focus on the western part of the system from the St Croix Basin to the Whiting Basin when the Anegada Passage extends to the Sombrero Basin to the NE. Understanding the whole system requires an extended data set.

Several tectonic models proposed different causes and types of deformation for the interpretation of the Anegada Passage formation including a NW-SE extension [e.g., *Feuillet et al.*, 2002], a sinistral transtension [e.g., *Mann and Burke*, 1984; *Raussen et al.*, 2013] or a dextral transtension [e.g., *Jany et al.*, 1990; *Masson and Scanlon*, 1991; *Mann et al.*, 2005]. These different models propose very different explanation and tectonic model probably due to the lack of bathymetry and penetrative seismic data. *Jany et al.* [1990] work between the Whiting Basin to St Croix Basin using bathymetry and seismic data acquired in 1985. *Raussen et al.* [2013] were interested in the Virgin Islands Basin using bathymetry and seismic data acquired in 2007. Other models were mainly conceptual with global understanding of the Lesser Antilles geodynamic [e.g., *Feuillet et al.*, 2002]. Thus, the Anegada Passage opening remains enigmatic, due to the limited available data in the area. In the northern Lesser Antilles forearc, the detailed bathymetry was incomplete and no deep seismic imagery had ever been acquired. In order to propose a global tectonic model of the area we examine the former studies and we complete with the new extensive data of Antithesis.

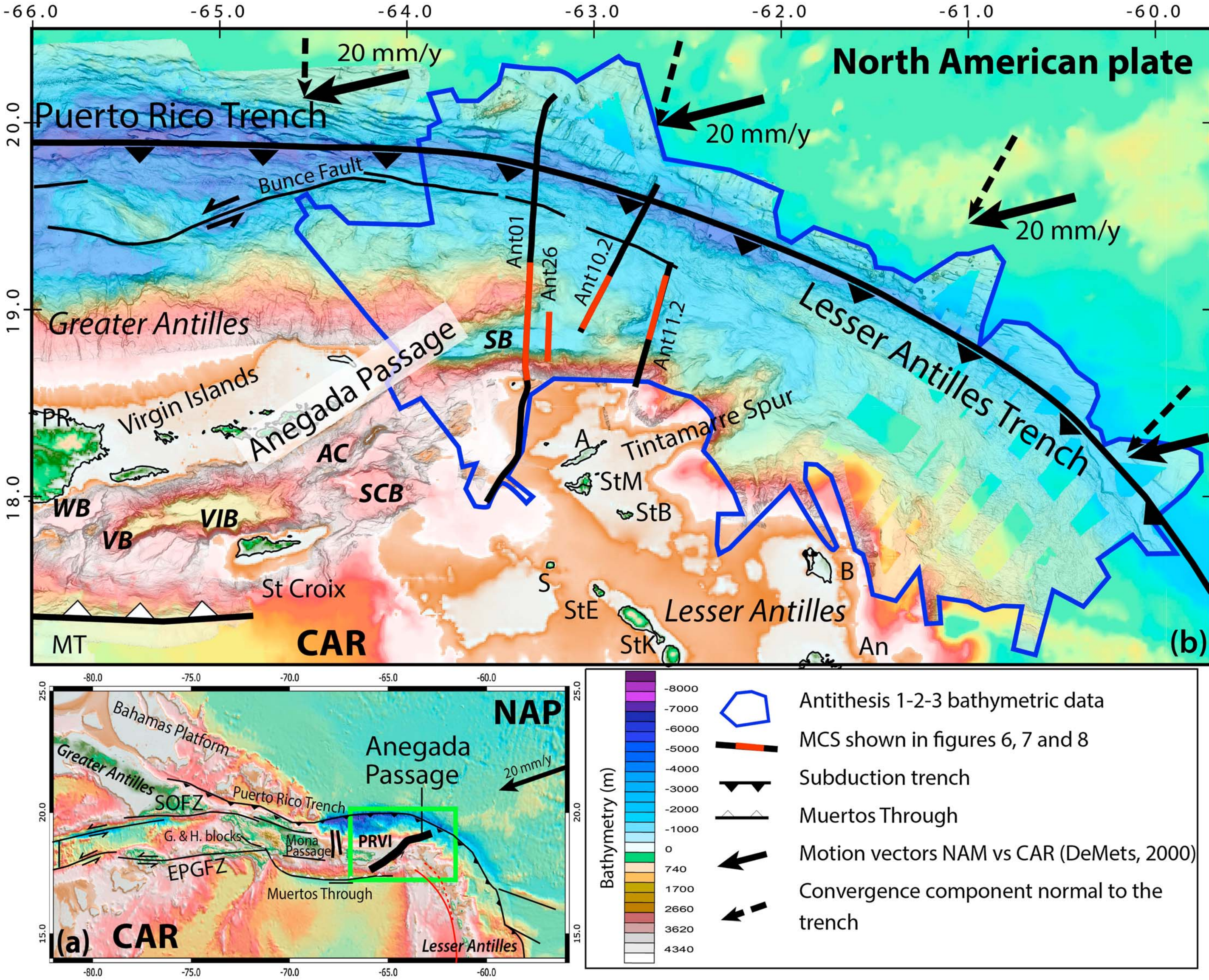

Figure 1. Bathymetric maps showing the geodynamic and tectonic settings of (a) the Caribbean Plate [*Leroy et al*., 2015; *Corbeau et al*., 2016] and (b) the Anegada Passage. The bathymetry is a compilation of data acquired during the Antithesis cruises (100 m grid resolution), data acquired during eight surveys between 2002 and 2013 [*Andrews et al*., 2013] (150 m grid resolution) and *Smith and Sandwell* [1997] altimetry-derived data (1′ grid resolution). Plain and dotted black arrows stand for convergence vector between the North American and the Caribbean Plates [*DeMets et al*., 2000] and convergence component normal to the trench, respectively. Note that the length of dotted arrows is not representative to the normal convergence component slip. The convergence obliquity increases northward. Green and blue contours, respectively, frame the study area for this paper in Figure 1a and for the Antithesis cruises in Figure 1b. A: Anguilla; An: Antigua; AC: Anegada Canyon/Anegada Passage (sensu stricto); B: Barbuda; CAR: Caribbean Plate; G&H: Gonave and Hispaniola; PR: Puerto Rico; S: Saba; SB: Sombrero Basin; SCB: St Croix Basin; StB: St Barthélemy; StE: St Eustace; StK: St Kitts; StM: St Martin; VB: Vieques Basin; VIB: Virgin Island Basin; and WB: Whiting Basin.

Cruises Antithesis 1 (November 2013–January 2014) Antithesis 2 (February–July 2015), and Antithesis 3 (May 2016) aim at studying the deep structure, the tectonic deformation, the seismic activity, and the thermal structure of the poorly investigated northern segment of the Lesser Antilles margin (Guadeloupe-Virgin Islands) (Figure 1b). Based on the bathymetric map and selected deep multichannel seismic (MCS) lines, we intend to shed a new light onto the tectonic evolution of the Anegada Passage in the geodynamic context of a margin segment that has undergone a past collision with the Bahamas Bank and an ongoing oblique subduction [*DeMets et al*., 2000]. We first focus on the structure and tectonic pattern of the newly imaged northeastern extent of the Anegada Passage in the Lesser Antilles forearc. We then discuss the implications of this newly imaged segment regarding to previously published tectonic scenario. At last, based on the

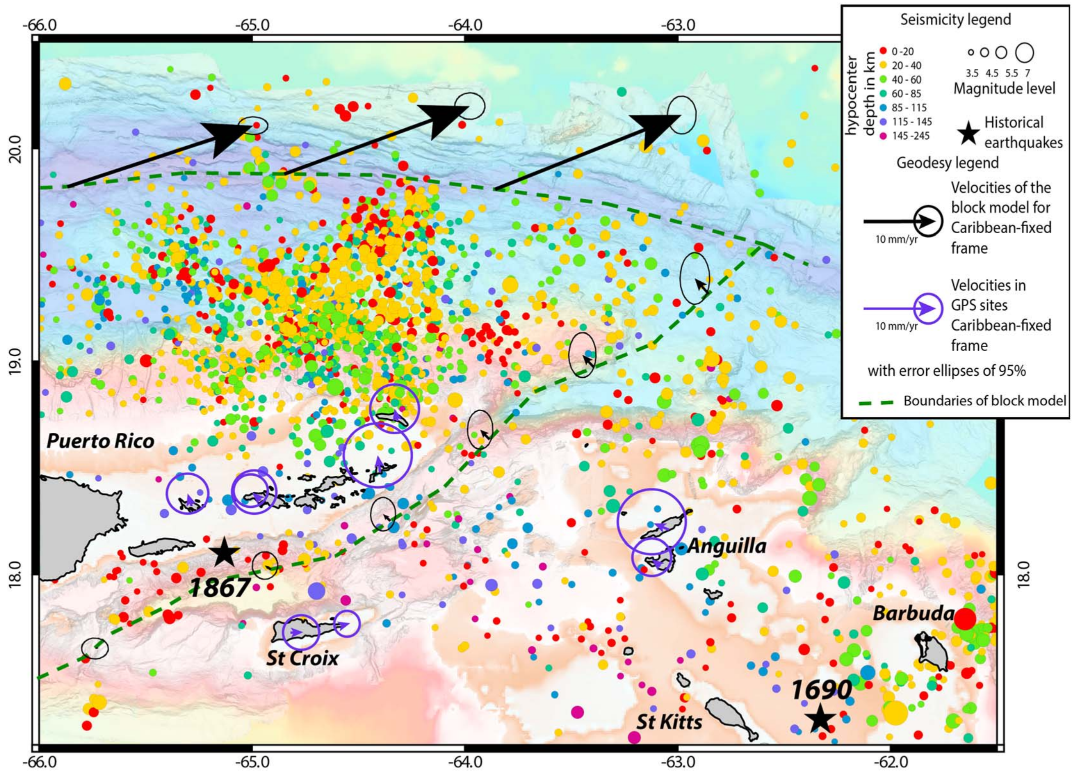

Figure 2. Seismicity location along the northern Lesser Antilles margin. The colored circles are the earthquakes from the PDE/NEIC catalog ($M_W > 3.5$ from 1900 to 2015), with size and color representing magnitude and epicentral depth, respectively. The black stars represent two historical earthquakes of 1690 and 1867; in the Caribbean fixed frame the purple arrows represent the plate velocities at GPS sites, and black arrows are the best fit kinematic block model [*Calais et al.*, 2016].

tectonic pattern of the basins sedimentary infill interpreted, thanks to these new seismic lines, we discuss the past and current tectonic evolution of the whole Anegada Passage spanning from the Southeast of Puerto Rico up to the Lesser Antilles trench.

2. Regional Settings

2.1. Geodynamic Setting

The North American Plate subducts below the Caribbean Plate with a convergence rate of 20 mm/y to the azimuth N254°E direction [*DeMets et al.*, 2000] (Figure 1) and is responsible for the 800 km long Lesser Antilles volcanic arc which extends from South America continent up to the Anegada Passage at the north-eastern tip of the Caribbean Sea. The convergence vector is similar over the northern Lesser Antilles while the subduction trench progressively rotates from a NNW-SSE direction offshore Guadeloupe to an E-W direction north of Virgin Islands. This rotation results in a northward increase of the convergence obliquity (Figure 1). To the north of Puerto Rico and Virgin Islands, the steep subvertical 535 km long Bunce Fault, which penetrates 5 km beneath the seafloor and soles out downward onto the subduction interface, likely accommodates left-lateral motion related to the convergence obliquity [*ten Brink et al.*, 2004].

Some authors, (*Byrne et al.* [1985] and *Mann et al.* [1995]), considered that the northern edge of the Caribbean Plate is possibly fragmented into three microplates, named Gonave, Hispaniola, and Puerto Rico-Virgin Islands (PRVI) (Figure 1).

The Anegada Passage (Figure 1a) is frequently interpreted as the southeastern tip of the PRVI crustal block [*Masson and Scanlon*, 1991] or microplate [*Byrne et al.*, 1985; *Mann et al.*, 1995; *Jansma et al.*, 2000]. The seismicity is scarce in the Anegada Passage area (Figure 2) and mostly located to the northwest over the Virgin Islands forearc and to the South of Barbuda Island. Recent geodetic studies reveal very low to

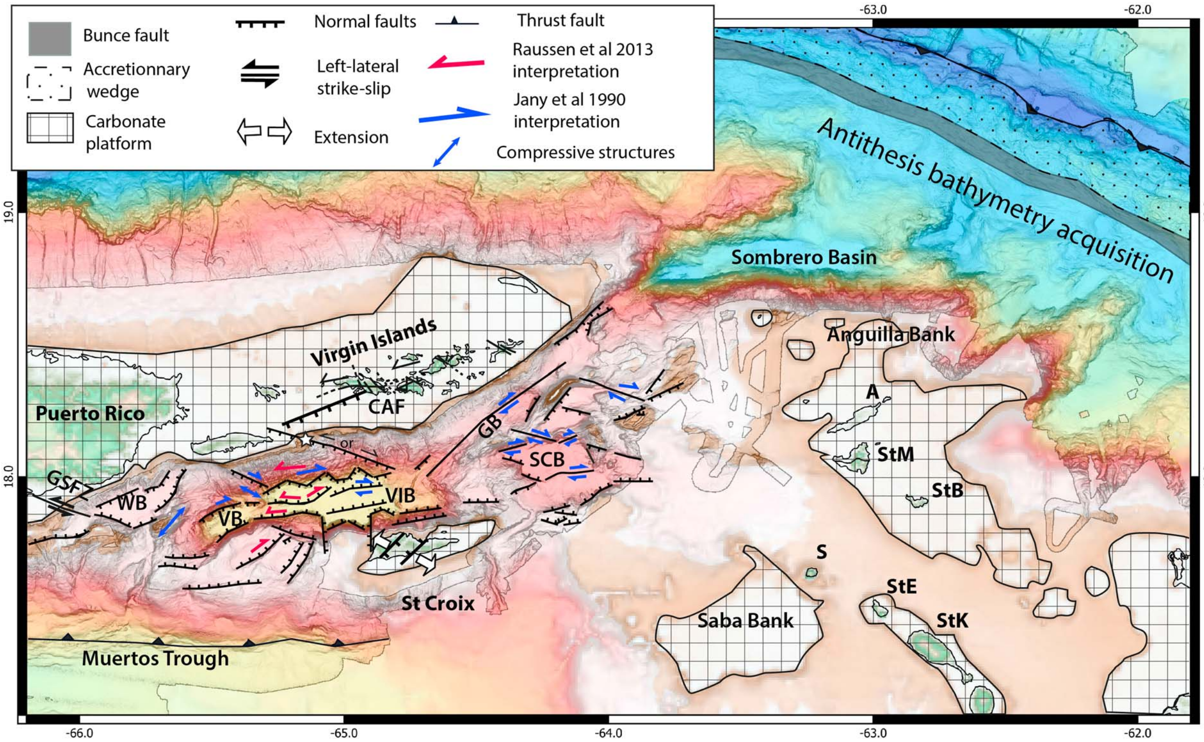

Figure 3. Morphotectonic interpretation of the Anegada Passage according to *Jany et al.* [1990] in blue and *Raussen et al.* [2013] in red. The white star is the 1867 M_W 7.2 earthquake. The bathymetry is on a compilation of recent multibeam data [*Andrews et al.*, 2013; *Marcaillou and Klingelhoefer*, 2013]. A: Anguilla; CAF: Charlotte Amalie Fault; GSFZ: Great Southern Fault Zone S: Saba; SCB: St Croix Basin; StB: St Barthélemy; StE: St Eustace; StK: St Kitts; StM: St Martin; VB: Vieques Basin; VIB: Virgin Islands Basin; and WB: Whiting Basin.

insignificant relative motion (Figure 2) across the Anegada Passage questioning the current existence and activity of this microplate limit [*Symithe et al.*, 2015].

2.2. The Anegada Passage Structural Context

The rhomboidal E-W trending Whiting, Vieques, Virgin Islands, and St Croix pull-apart basins (Figure 3) are fractured by N45° to N135° trending normal fault [*Holcombe*, 1978; *Jany et al.*, 1990; *Raussen et al.*, 2013], probably with strike-slip component. The Virgin Islands Basin is bounded to the north and the northeast by NW-SE to ENE-WSW trending strike-slip faults, possibly associated with positive flower structure (Figures 2 and 3). This basin is bounded to the south by E-W listric normal faults and N-S normal transfer faults [*Jany et al.*, 1990]. Two restraining bends, NE-SW and NW-SE directed, are located between the Whiting and Vieques Basins, and between the Vieques and Virgin Island Basins, respectively. Based on discontinuous data set, *Jany et al.* [1990] mostly interpreted NW-SE faults as normal, N80 to N100° trending faults as dextral strike-slip, and NW-SE trending faults as sinistral strike slip. Based on new bathymetric data within the Virgin Island Basin, *Raussen et al.* [2013] propose that E-W trending faults are normal, NNE-SSW to NE-SW trending faults are dextral strike slip, and E-W trending faults are mainly sinistral strike slip.

Thus, various structural investigations, onshore and offshore, highlighted some consistent tectonic patterns from the Whiting Basin to the Anegada Canyon: (1) E-W to NW-SE normal faults locally with sinistral or dextral strike-slip component; (2) strike-slip faults with different interpretations according to authors, dextral [*Jany et al.*, 1990], sinistral [*Raussen et al.*, 2013] with orientation ranging from N80° to N100°; (3) NW-SE to N-S restraining bends associated with positive flower structures, and (4) elongated basins with main axis trending in E-W direction. Through the western part of Anegada Passage, *Jany et al.* [1990] conclude to a ENE-WSW dextral strike-slip deformation while *Raussen et al.* [2013] to a ENE-WSW sinistral strike-slip deformation.

2.3. Anegada Passage Tectonic Models

Various authors proposed different tectonic models combining extension with right- or left-lateral strike-slip deformation (Figure 4).

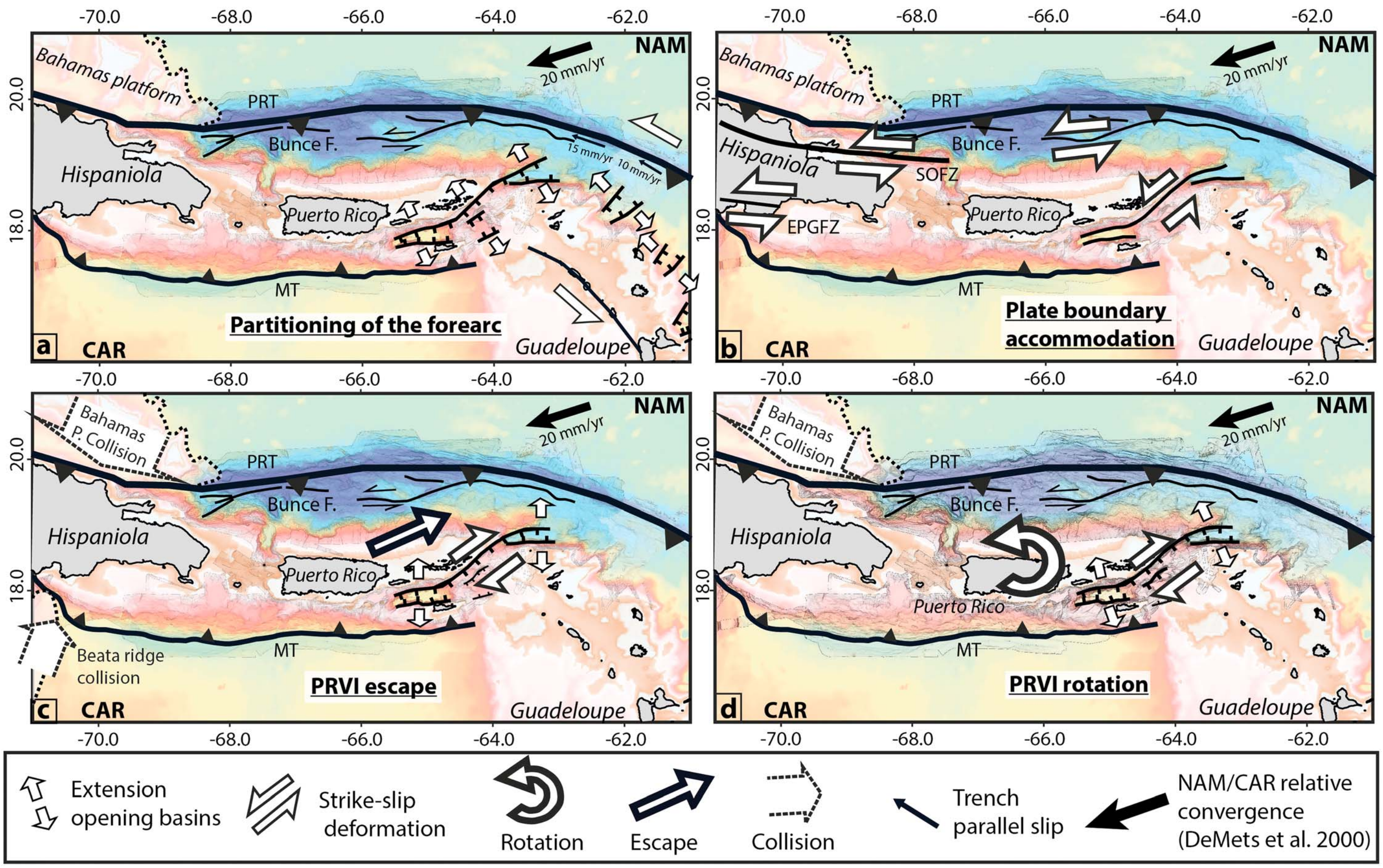

Figure 4. Four tectonic models for the Anegada Passage formation. (a) NW-SE pure extension across the Lesser Antilles forearc due to the partitioning [e.g., *Feuillet et al.*, 2002], (b) left-lateral strike-slip fault due to the accommodation of deformation in a diffuse plate boundary [*Mann and Burke*, 1984; *Van Benthem et al.*, 2014], (c) right-lateral transtension due to the PRVI escape toward the northeast, [e.g., *Jany et al.*, 1990], (d) NW-SE extension associated to a right-lateral strike-slip fault due to the rotation of PRVI microplate [e.g., *Masson and Scanlon*, 1991; *Mann et al.*, 2005].

1. In the northern Lesser Antilles forearc, the NE-SW trending valleys bounded by spurs between Antigua and Saint Barthelemy Islands are approximately parallel to the Anegada Canyon. These valleys are possibly bounded by normal faults, subperpendicular to the trench that would indicate a NW-SE extension [e.g., *Feuillet et al.*, 2002]. These authors propose that the strain partitioning related to the subduction obliquity caused this NW-SE extension and therefore the Anegada Passage opening (Figure 4a).
2. According to *Mann and Burke* [1984], the Anegada Passage consists of pull-apart en échelon basins resulting from this left-lateral strike-slip deformation (Figure 4b). In such interpretation, the area between Puerto Rico Trench and Muertos Trough could be interpreted as a diffuse plate boundary [*Mann and Burke*, 1984; *Van Benthem et al.*, 2014] accommodating the oblique convergence with a large left-lateral strike-slip faults system including the Enriquillo-Plaintain Garden Fault Zone (EPFGZ) and the Septentrional-Oriente Fault Zone (SOFZ).
3. The successive collisions during Miocene of the Bahamas Platform and the Beata Ridge against the Caribbean Plate in the Puerto Rico Trench possibly result in an ENEward escape of the PRVI block accommodated by right-lateral strike-slip deformations along the Anegada Passage [e.g., *Jany et al.*, 1990] (Figure 4c).
4. Paleomagnetic data suggest a 25° counterclockwise rotation of the PRVI block between 11 Ma and 4.5 Ma [*Reid et al.*, 1991]. This rotation, probably caused by the Bahamas Plateform collision, triggered a right-lateral strike-slip movement and NW-SE extension in the Anegada Passage [e.g., *Masson and Scanlon*, 1991; *Speed and Larue*, 1991; *Mann et al.*, 2005] (Figure 4d).

The models 1 and 2 result from the partitioning due to the obliquity of the subduction evolving since Eocene [e.g., *Feuillet et al.*, 2002]. The tectonic deformation within models 3 and 4 results in the Miocene main

Table 1. Acquisition Parameters for the Selected MCS Lines in This Paper

Seismic Lines	Ant01–Ant11.2	Ant10.2	Ant26
Cruise	Antithesis I	Antithesis I	Antithesis III
Airgun array	7699 in^3	7699 in^3	3902 in^3
Fire rate	1 shot/1 mn	1 shot/1 mn	1 shot/30 s
Shot spacing	150 m	150 m	75 m
Traces number of the streamer	300	288	720
Data sampling	2 ms	2 ms	2 ms
Traces spacing	12.5 m	12.5 m	6.25 m
Fold coverage	12 fold coverage	12 fold coverage	30 fold coverage
Acquisition speed	5 knots	5 knots	5 knots

docking of the Bahamas Bank to the northern margin in a context of oblique subduction. A recent interpretation of geodetic data indicates very slow to insignificant current relative motion across the Anegada Passage (Figure 2) [*Symithe et al.*, 2015; *Calais et al.*, 2016]. The authors suggest that the morphotectonic pattern of the Anegada Passage is not representative of current geodynamics but of a major past tectonic event [*Calais et al.*, 2016] which is the collision of Bahamas Bank against the northern margin but for *Leroy et al.* [2000] and *Jany et al.* [1990] also the tectonic escape of the Caribbean plate toward the east.

3. Data Acquisition and Processing

During the survey Antithesis 1 (December 2013) and Antithesis 3 (May 2016), on board the R/V *L'Atalante* and *Pourquoi Pas*?, we recorded 54 multichannel seismic lines (MCS), four wide-angle seismic profiles (WAS), subbottom profiles (CHIRP), and multibeam swath bathymetry (Figure 1). The acquisition parameters for the selected MCS lines in this paper are summarized in Table 1.

The quality control and the binning of the MCS data were performed on board using QCSispeed® (Ifremer) and SolidQC® (Ifremer), and the processing was performed using GEOCLUSTER®.

The processing sequence includes the following: a 4 ms data sampling, a band-pass filtering (2–7–60–80 Hz), an FK filtering in order to reduce linear noises, amplitude attenuation for noisy traces due, for example, to streamer birds, a predictive deconvolution to improve the image resolution, velocity analysis and Normal Move-Out (NMO) correction, external mute to remove the direct and refracted waves before NMO and after NMO to reduce the far offset stretching of the shallow reflections, internal mute to reduce the primary multiple amplitude, and velocity stack. As the acquisition is at deep water depth, we applied a poststack frequency-wavenumber migration at constant water velocity of 1520 m/s. The Antithesis multibeam bathymetry data were processed on board using the Caraibes software® (Ifremer). It consisted in ping editing and a 100 m gridding using a near-neighbor method. We use 100 m and 150 m grids for close and large view, respectively.

4. Results and Interpretation of the Marine Geophysical Data

In the following, we present our images and interpretations of the tectonic deformation pattern in the northern Lesser Antilles margin based on multibeam data (Figure 5) and the selected MCS lines Ant01, Ant26 (Figure 6), Ant10.2 (Figure 7), and Ant11.2 (Figure 8). No automatic gain control (AGC) was used for the visualization of the MCS profiles presented here.

4.1. The Sombrero Basin

The E-W trending Sombrero Basin is an 87 km long, 25 km wide, and up to 6300 m deep depression located to the northeast of the Anegada Canyon (Figure 5). This rhomboidal to S-shaped basin is divided into three subbasins, labeled Sb1, Sb2, and Sb3 from southwest to northeast.

4.1.1. Seismic Units

Based on seismic unconformities, acoustic features, and deformation style, we identify from bottom to top five main seismic units, SA, SB, SC, SD, and SE (Figure 6). *Vp* velocity estimated from wide-angle modeling is more than 5.5 km/s for the top of unit SA and 2.2 to 3.5 km/s for units SB to SD, thus supporting their

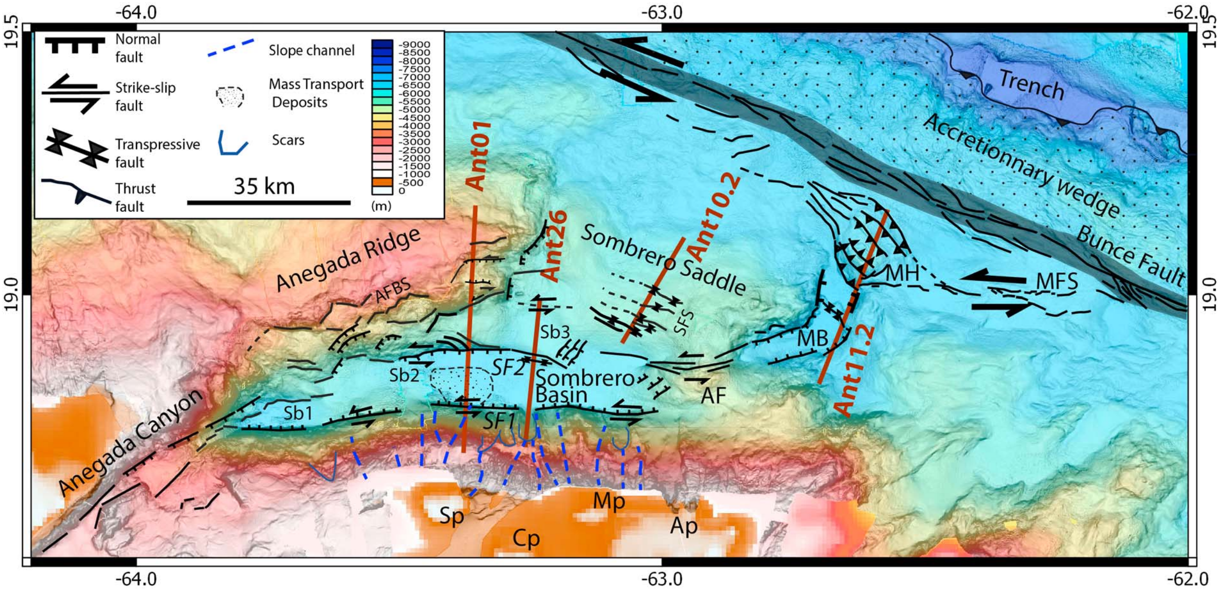

Figure 5. Interpretation of multibeam data in the northern Lesser Antilles margin. AF: Anguilla Fault, Ap: Anguilla Platform, AFBS: Anegada Faults and Basin System, Cp: Crocus Platform, MB: Malliwana Basin, MFS: Malliwana Faults System, MH: Malliwana Hill, Mp: Malliwana Platform, Sb1-Sb2-Sb3: three Sombrero subbasins. Sp: Sombrero platform.

mafic and sedimentary nature, respectively [*Laurencin et al*., 2015]. The following description supports the interpretation that these main seismic units recorded a past extensive to transtensive tectonic phase with SB, SC, and SD being preextension, syn-extension, and postextension tectonic sedimentary units.

1. In lines Ant01 and Ant26 (Figure 6) unit SA is poorly reflective with locally poorly organized high-amplitude reflectors. The contrast with the overlying layered seismic units and the high velocity *Vp* indicate that unit SA corresponds with the acoustic basement beneath the Sombrero Basin.
2. Unit SB consists of low-amplitude, low-frequency, layered, discontinuous, and deformed reflectors. High-amplitude reflectors SB1 and SC1 limit, respectively, unit SB at the base and at the top. Although the SB1 continuity is unclear, unit SB thickness, ~1 stwt in Sb2 (line Ant01-CMP 11200–12100) and ~1.2 stwt in Sb3 (line Ant26 – CMP 2100–2900) does not significantly vary from south to north and laterally in the Sombrero Basin. Unit SB interpretation in Sb2 (line Ant26–CMP 1100–2000) is unclear, although high-amplitude reflector portions, possibly corresponding with SB1 and SC1, limit a ~ 2 stwt thick layer, which is consistent in depth and seismic features with SB in Sb2 (line Ant01) and Sb3 (line Ant26). Unit SB would therefore correspond to the preextension sedimentary unit.
3. Unit SC is characterized by a northward dipping fan-shaped geometry. Continuous, layered, high-amplitude reflectors of unit SC differ from the discontinuous reflectors of the underlying units. In Sb2 (line Ant01), SC thickens from 0.2 stwt at CMP 12000 to 1.4 stwt at CMP 11300. Consistently in line Ant26, unit SC, although poorly reflective likely thickens from ~0.8 stwt at CMP 1100 to ~2 stwt at CMP 1800 with a northward dipping fan-shaped geometry. Despite the poor resolution at depth in line Ant26, the similarity and proximity of lines Ant01 and Ant26 in Sb2 suggest a lateral continuity of the northward dipping fan-shaped geometry for SC. In Sb3 (line Ant26), SC thickens from 1 stwt at CMP 2800 to 2 stwt at CMP 2000 with a southward dipping fan-shaped geometry. Locally in line Ant01, 0.3 stwt thick unit SCa of shattered and disorganized reflectors tops unit SC and has no lateral equivalent in line Ant26. This local chaotic unit SCa between layered units, at the canyon mouth, is likely to be a Mass Transport Deposit. Unconformity SC1, between homogeneously thick unit SB and fan-shaped unit SC, corresponds with a drastic change in the tectonic setting within the Sombrero Basin and would therefore correspond to the syn-extensional phase.
4. Unit SD is characterized by rather horizontal deposits. This unit SD is a 0.4–0.6 stwt thick series of layered continuous, high-amplitude high-frequency reflectors. In Sb2 (line Ant01), SD reflectors, slightly dipping southward, prograde in the basin and downlap onto high-amplitude reflector SD1, the seismic unconformity at the base of SD. In Sb2 (line Ant26) SD reflectors are horizontal and lap laterally onto unconformity

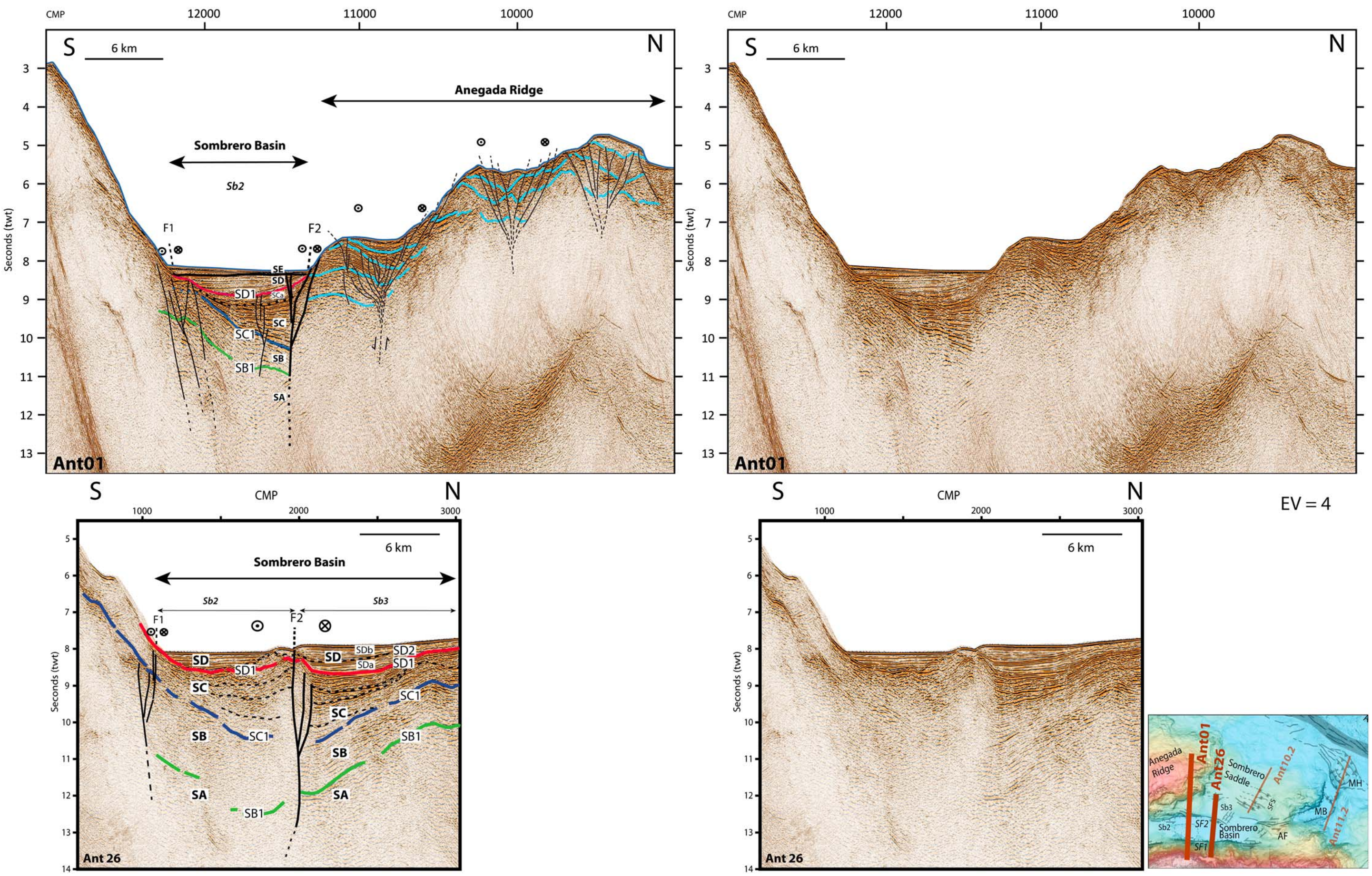

Figure 6. Uninterpreted and interpreted seismic lines Ant01 and And26. These N-S trending lines that image subbasins Sb2 and Sb3 within the Sombrero Basin are parallel and separated by 26 km (location in Figure 5). SB1 (green), SC1 (blue), SD1 (red) are, respectively, the upper discontinuity of units SA, SB, and SC. SA is the acoustic basement. SB, SC, and SD are, respectively, preextension, syn-extension, postextension deformation tectonic sedimentary units. The main reflectors of the Anegada Ridge are drawn in light blue.

SD1 at the basin flanks. In Sb3 (line Ant26), unit SD is divided into two subunits SDa and SDb, with the deepest reflectors, lapping southward onto basal unconformity SD1. Sda is the thickest, 0.5 stwt, at CMP 2600, where unconformities SD1, SD2, and internal reflectors of SDa dip consistently southward. In contrast SDb is the thickest, 0.4 stwt, at CMP 2200, where the internal reflectors, the discontinuities, and the seafloor are horizontal, indicating a southward migration of the depocenter. Unit SD would therefore correspond to the postextensional phase.

5. In line Ant01, the shallowest sedimentary unit SE is 0.2 stwt thick at CMP 11900 near the southern wall of the Sombrero Basin and thins northward, topped by the gently northward dipping seafloor. This unit is located near a gully in the southern wall of the Sombrero Basin and corresponds with a sedimentary lobe in the bathymetry (Figure 5). This unit observed locally in line Ant01 is thus possibly related to gully-driven sediment supply.

Thus, in Sb2 and Sb3 subbasins, fan-shaped seismic unit SC overlies dipping and homogeneously thick unit SB and is overlain by subhorizontal blanketing unit SD. This suggests a past extensive to transtensive tectonic phase with SB, SC, and SD being preextension, syn-extension, and postextension tectonic sedimentary units.

4.1.2. Tectonic Pattern

4.1.2.1. F1 Fault Interpretation

An E-W 25° steep wall marks out the Sombrero Basin to the south, connecting the deep basin with the shallow Sombrero, Crocus, Malliwana, and Anguilla carbonate platforms (Figure 5). At depth northward dipping steep planes truncate reflectors of units SC, SB, and possibly SA (Figure 6). These fault planes converge downward possibly soling out onto a major fault drawing a flower structure. Reflectors of units

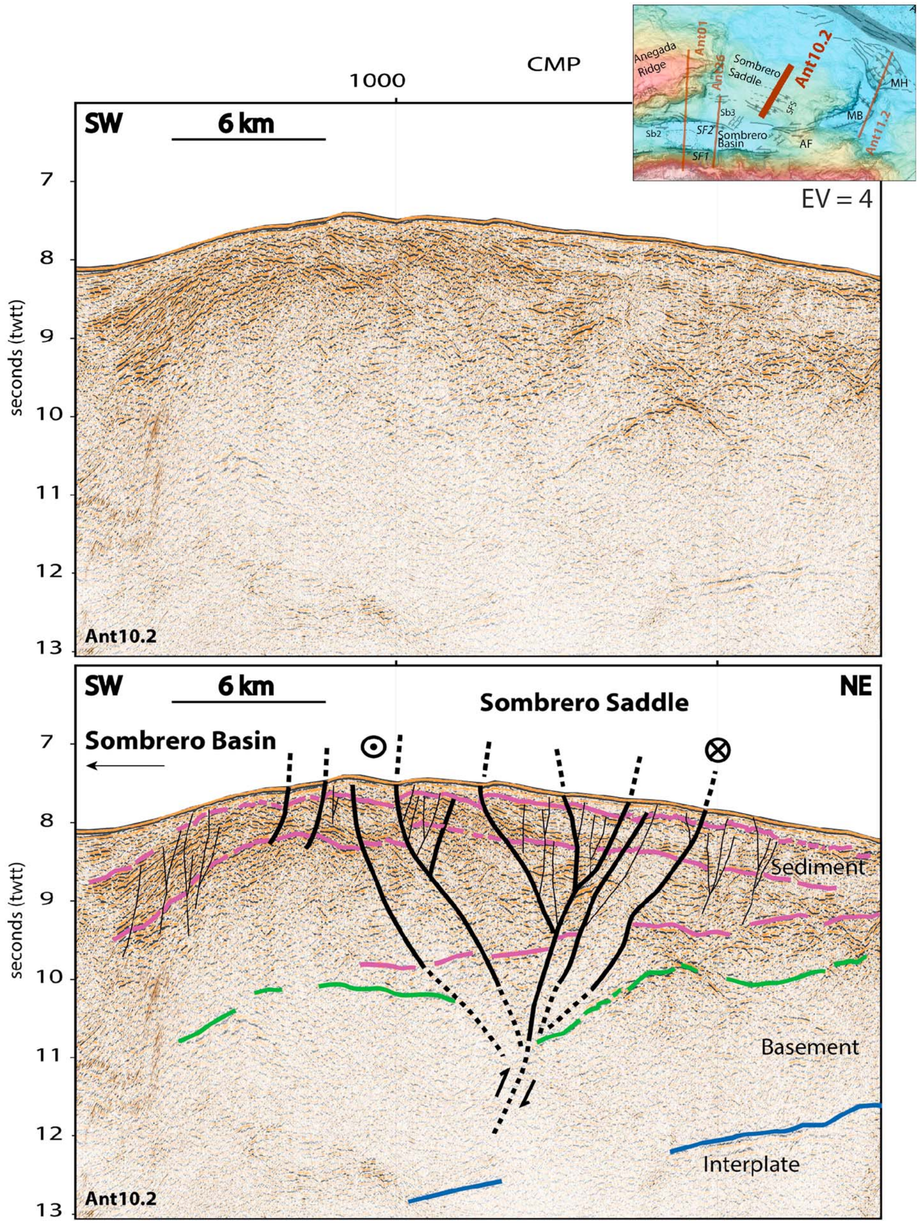

Figure 7. Uninterpreted and interpreted section of line Ant10.2 across the Sombrero Saddle. A major positive flower structure outcrops at the Sombrero Saddle seafloor where it corresponds with NW-SE lineaments. Interplate, top of the basement, and the main reflectors in the sedimentary unit are, respectively, drawn in blue, green, and purple.

SB and SC are frequently tilted northward along these fault planes without showing a significant vertical shift. These steep faults in negative flower structure, F1, associated with a rectilinear, steep, 85 km long, EW trending scarp that marks out the Sombrero Basin to the South, are likely to be a strike-slip fault zone possibly transtensive.

4.1.2.2. F2 Fault Interpretation

Line Ant01 images the E-W trending, 40 km long, and subvertical steep south facing wall that marks out the Sombrero subbasin Sb2 to the north and connect it with the Anegada Ridge (CMP 10800 to 8000 for line Ant01) and the shallow Virgin Islands platform. At depth beneath this northern wall, a steep southward dipping plane F2 limits the reflectors of deep seismic units SB and SC. Reflectors of SB are parallel and dip homogeneously toward F2, while the fan-shaped geometry of SC faces F2. It suggests transtensive fault.

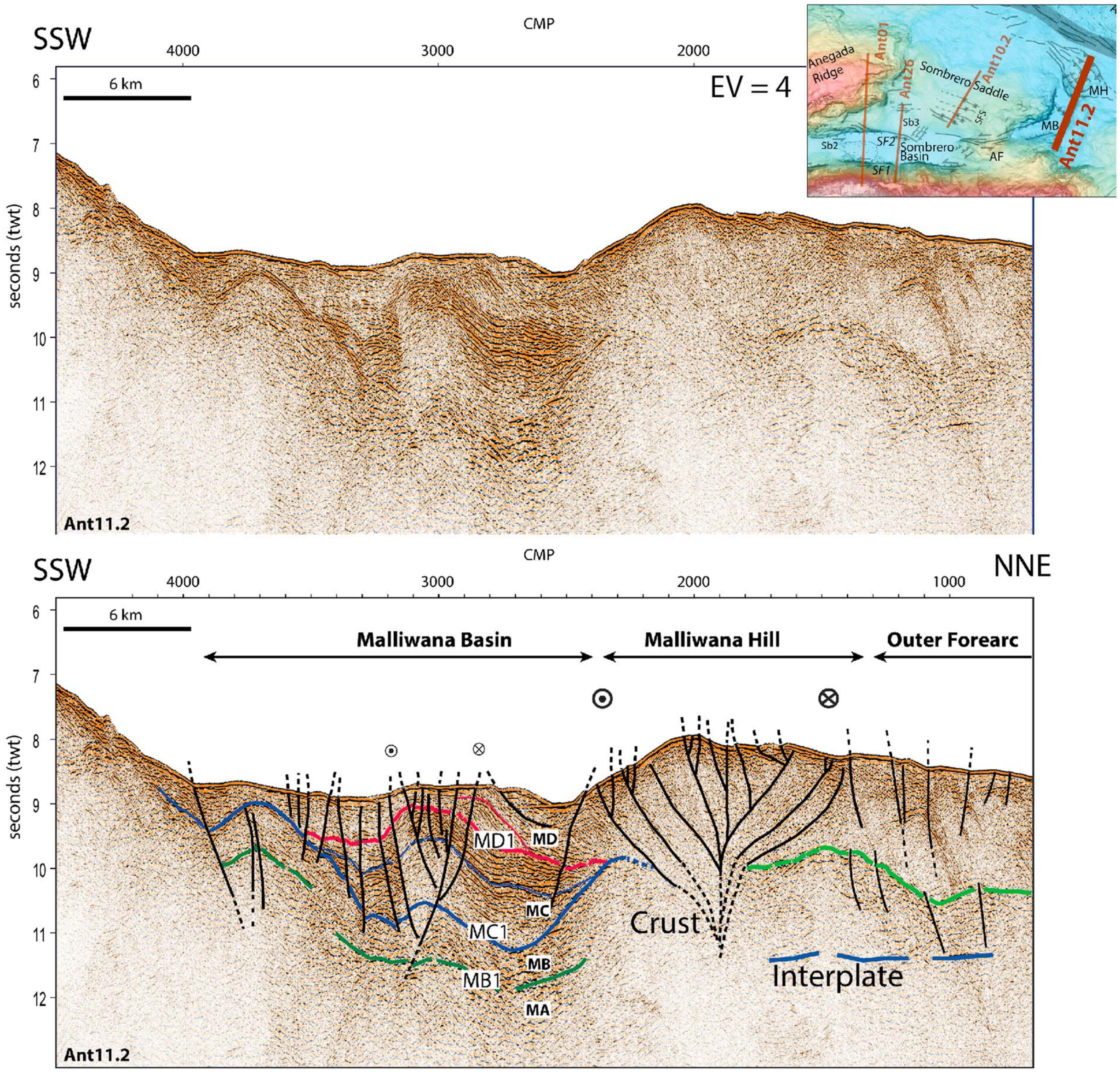

Figure 8. Uninterpreted and interpreted seismic line Ant11.2 across the Malliwana Basin, the Malliwana Hill, and the outer forearc. MB1 (green), MC1 (thick blue), and MD1 (thick red) are the upper limit of units MA, MB, and MC. In the Malliwana Basin, within the outer forearc, blue and green lines, respectively, correspond to the interplate and the top of basement.

In line Ant01, fault F2 is located near the steep Anegada Ridge flank, whereas in line Ant26, F2 is located at the smooth transition between subbasins Sb2 and Sb3. Near F2, between CMP 1800–2200 in line Ant26, upper reflectors of SC, reflectors of SD, and unconformities SD1 and SD2 are uplifted and folded. These deformed reflectors are truncated by steep to subvertical fault planes converging downward and drawing a positive flower structure. In line Ant26, this strike-slip tectonic deformation is associated to a seafloor high that divides Sb2 from Sb3, while the seafloor is flat above F2 in line Ant01. The bathymetric data reveal a slight change in F2 direction from E-W in line Ant01 to WNW-ESE in line Ant26. The direction variation possibly influences the F2 tectonic pattern that is strike slip in line Ant01 and transpressive in line Ant26.

The Sombrero Basin is a typical rhomboidal basin bounded by approximately E-W left-stepping en échelon transtensive faults (F1 and F2 faults) and NE-SW scarps. F2 is associated to fan-shaped sedimentary unit SC. F2 faults change slightly of direction associated with positive flower structure affecting sediments with folded, uplifted shallower unit SD and a topographic high. It is consistent with transpressive deformation.

4.2. The Anegada Ridge

The 110 km long, 45 km wide NE-SW Anegada Ridge is located to the East of the Virgin Islands carbonate platform (Figure 1). Along the southern flank of the ridge, E-W and NE-SW scarps mark out 10 km long rhomboidal-shaped left-stepping en échelon depression, between 63°20′ and 63°50′ of longitude (Figure 5).

Seismic line Ant01 images the easternmost part of the Anegada Ridge. Between CMP 9000 and 11000 (Figure 6), the southern flank of the Anegada Ridge shows steep slope dividing flat seafloor zones (from CMP 10800 to 11000 and from 9800 to 10200) that correspond with the easternmost rhomboidal depressions. Several steep planes, dipping either southward and northward, truncate reflectors that are mostly shifted downward in the direction of the fault dip. These steep faults with normal throw penetrate the upper part of the margin basement apparently converging downdip forming negative flower structure, which suggest transtensive deformation. Thus, at the eastern end of the Virgin Islands carbonate platform, the Anegada Ridge southern flank is incised by four en échelon left-stepping rhomboidal depressions bounded by E-W and NE-SW scarps and associated to transtensive fault that we call the Anegada Fault and Basin System (AFBS).

4.3. The Sombrero Saddle

The Sombrero Saddle at the northeastern limit of the Sombrero Basin contrasts with the Anegada Ridge with a water depth greater than 5700 m and a low angle ($<3°$) topographic slope. On the seismic line Ant10.2 (Figure 7), from CMP 800 to 2000, at depth of 7.5 to 9 stwt, steep to vertical planes dipping southwestward and northeastward truncate the reflectors shifting them upward in the direction of the faults dip. Moreover, some faults outcrop, fracturing and uplifting the seafloor and drawing NW-SE lineaments in the bathymetry (Figure 7). These faults with reverse throw converge at depth toward the acoustic basement reflector, resulting in a positive flower structure. Thus, the Sombrero Saddle, to the east of the Anegada Ridge, is deeply fractured by a steep likely transpressive faults zone located within the forearc crust.

4.4. The Anguilla Fault

To the southeast of Sombrero Saddle and to the northeast of Sombrero Basin a ~ 20 km long E-W trending lineament is visible on the bathymetric map at latitude 18.9°N and longitude $-63°$. This lineament is located in the continuity of Fault F2 in the Sombrero Basin (Figure 5). Thus, it is likely to be a segment of the strike-slip faults zone called Anguilla Fault that ties the Sombrero Basin to the Malliwana Basin (Figure 5).

4.5. The Malliwana Basin

The 6900 m deep Malliwana Basin is approximately 30 km long and 6 km wide located to the northeast of the Sombrero Basin. The main basin axis rotates from a WSW-ENE direction in the western part of the basin to a SW-NE direction in the eastern part.

4.5.1. Seismic Units

Even if the seismic profile is located on the edge of the Malliwana Basin, we interpret four major seismic units MA, MB, MC, and MD from bottom to top based on seismic unconformities between CMP 2500 and 4000 in line Ant11.2 (Figure 8):

1. Unit MA, globally diffracting with scarce poorly organized high-amplitude reflectors is interpreted as the acoustic basement.
2. Unit MB consists of high-amplitude, low-frequency discontinuous reflectors. Low-frequency, high-amplitude discontinuous reflector MB1 divides this layered unit from underlying diffracting MA. MB is uniformly 0.7–0.9 stwt thick.
3. Unit MC consists of low-frequency, high-amplitude continuous reflectors except between CMP 2800 and 3200 where reflectors are discontinuous and low amplitude. MC reflectors lap southward and northward onto rising high-amplitude reflector MC1. This basal unconformity limits MC deposit between CMP 2400 and 3500. MC is 1.5 stwt thick from CMP 2650 to 3200 and pinches out at the basin limits at CMP 3550 and 2300.
4. Low-amplitude, high-frequency reflectors of unit MD differ from the high-amplitude underlying unit. MD reflectors downlap northward onto MD1 at CMP 2400–2800 and lap southward onto MC1 at CMP 3500–3700. MD is 0.3 stwt thick at the basin axis, CMP 2900–3150, and thickens northward and southward to 1.1 stwt.

4.5.2. Tectonic Pattern

Unit MB extends beneath the Malliwana Basin showing minor variations in thickness. MB internal reflectors, basal, and upper unconformities, MB1 and MC1, dip along the basin flank toward the basin axis. In contrast, MC deposit considerably thickens at the basin axis pinching out at the basin boundaries. MC and MD are folded without any evidence of syn-sedimentary deformation. At the fold axis, CMP 2700–3200, the seafloor is uplifted corresponding with a NW-SE trending lineament in the bathymetry. Steep fault planes that dip toward north and south converge downward drawing a positive flower structure at the fold axis. These fault planes (Figure 8) outcrop at the seafloor and possibly extend deep in the margin basement. This deformation pattern suggests that a past tectonic phase, mostly extensive, opened the Malliwana Basin before and possibly during unit MC deposit. Although fan-shaped sequences are not observed in the line direction, we do not rule out syn-sedimentary opening. Currently active transpression has deformed the basin since MC and possibly during MD deposit. The Malliwana Basin structure thus depicts a polyphased tectonic history made of a past extensive to transtensive phase followed by a recent and currently active transpressive phase.

4.6. The Malliwana Hill

To the north of the Malliwana Basin, the ~15 km eye-shaped, 700 m high poorly reflective Malliwana Hill is located between CMP 1400 and 2400 in line Ant112 (Figure 8). Steep planes that structure this topographic high converge downward to CMP 1800 in line Ant112 and possibly extend to the interplate contact. These planes outcrop at the seafloor generating topographic scarps, as for example at CMP 2220 1890, 1850, and 1680. The Malliwana Hill marks out the north the Malliwana Basin seismic units and to the south the deep reflections of the Lesser Antilles outer forearc (Figure 8). Locally, these steep planes truncate and shift sparse reflectors with apparent reverse throw. To the southeast of the Malliwana Hill, an E-W trending, 60 km long series of bathymetric lineaments, called Malliwana Fault System (MFS), extend from the hill southern flank to the Bunce Fault. Some bathymetric lineaments also extend northwestward from the northern hill flank.

This tectonic pattern indicate a 700 m high positive NW-SE flower structure (Figure 8) associated to en échelon strike-slip faults, which testify for transpressive deformation.

5. Discussion

5.1. The Anegada Passage Eastern Segment

The new data set acquired during cruises Antithesis 1 and 3 highlights the tectonic deformation pattern in the northern Lesser Antilles forearc domain, where we observed for the first time the eastern segment of the Anegada Passage.

From the Anegada Canyon to the Bunce Fault, prominent E-W trending left-stepping en échelon strike-slip faults (F1, F2, Anguilla Fault, and Malliwana Fault System) mark out and connect the basins (Figure 9a). The interpreted transtensive faults F1 and F2 mark out the deep, rhomboidal and E-W-elongated Sombrero Basin to the south and to the north. The transtensive Anguilla Faults mark out the narrow S-shaped Malliwana Basin to the south and extends westward to the Sombrero Basin. The Malliwana Faults System marks out the Malliwana Basin to the north and extends westward to the Bunce Fault and the accretionary wedge. Authors proposed similar descriptions for the Marmara Sea [e.g., *Armijo et al*., 2005] and the Dead Sea [e.g., *Garfunkel and Ben-Avraham*, 1996] basins and as results for analogue modeling [e.g., *McClay and Dooley*, 1995; *Wu et al*., 2009]. According to these results, the Sombrero and Malliwana basins are likely to be pull-apart basins mainly bounded by NE-SW scarps and normal faults as well as E-W strike-slip transtensive faults.

Similarly, the Anegada Faults and Basin System (Figure 9a) that incises the southern flank of the Anegada Ridge is a set of en échelon rhomboidal depressions bounded by E-W and NE-SW outcropping transtensive faults (Figures 5, 6, and 9). These E-W trending structures are likely to be a secondary pull-apart system subparallel and consistent with the main Sombrero-Malliwana system.

Several compressive to transpressive tectonic structures uplift the seafloor along WNW-ESE bathymetric lineaments associated to positive flower structure at depth in the Sombrero Basin, the Sombrero Saddle, and the Malliwana Basin (Figure 9a). The Malliwana Hill associated with the Malliwana Faults System to the south and to diffuse strike-slip faults to the north shows features of a restraining bend. Similar deformations

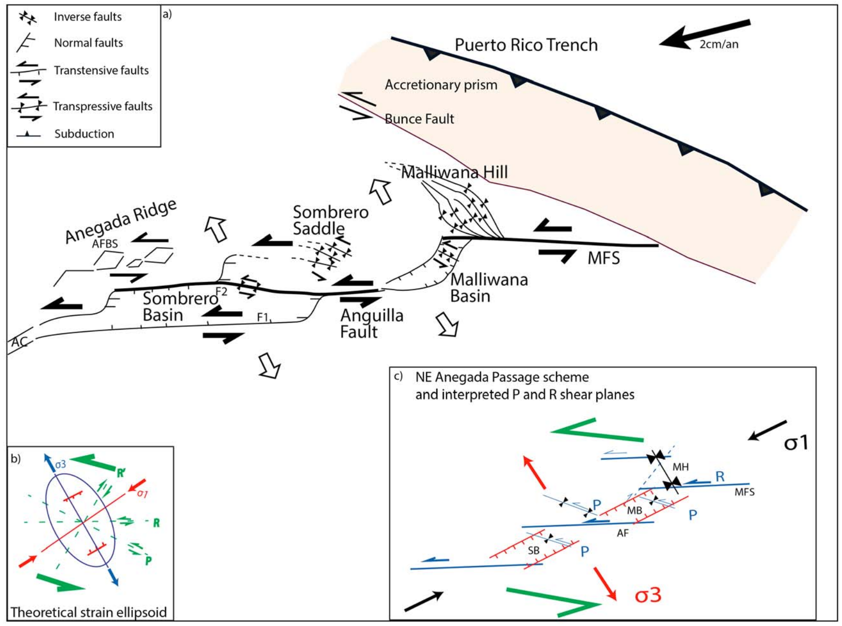

Figure 9. (a) Global tectonic interpretation of the eastern segment of the Anegada Passage. (b) Theoretical strain ellipsoid. (c) NE Anegada Passage scheme and interpreted P and R shear planes. AC: Anegada Canyon; AFBS: Anegada Faults and Ridge System; MFS: Malliwana Faults System.

were described along the San Andreas strike-slip fault [*Harding*, 1976; *Sylvester and Smith*, 1976; *Sylvester*, 1988] and in analog modeling results [*McClay and Bonora*, 2001].

Thus, the eastern Anegada Passage is a left-stepping en échelon system of strike-slip faults, pull-apart basins, and compressive to transpressive structures (Figure 9a). Strike-slip deformation frequently generates similar en échelon strike-slip faults separated by step over structures (pull-apart basins and restraining bend) as described along the Anatolian and the Alpine faults [e.g., *Barnes et al*., 2001] and in exhaustive study cases [*Christie-Blick and Biddle*, 1985; *Sylvester*, 1988]. The spatial organization of left-stepping strike-slip faults and related transpressive and transtensive step overs indicates a sinistral slip along the prominent E-W faults.

NW-SE to WNW-ESE trending compressive structures indicate a NE-SW compressive $\sigma 1$ axis. Consistently, most of the normal faults are striking NE-SW, thus indicating a NW-SE extensive $\sigma 3$ axis, perpendicular to $\sigma 1$ (Figure 9b–9c). In strike-slip systems, early and prominent R shear planes develop at a 30° angle to $\sigma 1$ [*Fossen*, 2010], later P shear planes favor compressive strike-slip faults at a 30° angle to $\sigma 3$ [*Burg*, 2013] while antithetic R′ shear planes are generally poorly developed in nature [*Sylvester*, 1988] (Figure 9b). The orientation and sinistral deformation of R and P planes, in the theoretical ellipsoid, are consistent with the observed prominent E-W sinistral strike-slip faults and NW-SE transpressive strike-slip faults, respectively. As a result, the observed deformation pattern along the eastern Anegada Passage is mostly consistent with a WNW-ESE sinistral strike-slip strain ellipsoid (Figure 9b).

5.2. The Anegada Passage: A Sinistral Strike-Slip System

Structural studies to the southwest of the Sombrero Basin resulted in comparable models [*Jany et al*., 1990; *Raussen et al*., 2013]. These authors interpret the Whiting, Vieques, Virgin Islands, and St Croix Basins (Figure 3) as narrow, E-W elongated pull-apart basins mainly bounded by E-W left-stepping en échelon strike-slip faults. On land, several ~E-W trending left-lateral strike-slip faults were described across the Virgin Islands [*Vila et al*., 1986] and Puerto Rico [*Jany et al*., 1990]. Thus, the direction of the pull-apart basin axis and the main strike-slip faults is consistent within the western and eastern segment of the Anegada Passage.

However, tectonic interpretations by *Jany et al*. [1990] and *Raussen et al*. [2013] in the western segment significantly differ from each other and from the proposed strain ellipsoïd for the eastern segment. Mostly based on bathymetric data and poorly resolved seismic lines, *Jany et al*. [1990] interpreted a NE-SW directed $\sigma 1$, N80–100 dextral P and R shear planes indicating a WSW-ENE mainly dextral strike-slip strain. However, *Raussen et al*. [2013] proposed a drastically different tectonic interpretation for the same study area. According to these authors, $\sigma 1$ is E-W, $\sigma 3$ is N-S, and the sinistral synthetic R shear planes are WSW-ENE indicating that the main strike slip is sinistral in a WSW-ENE direction. Thus, this recently revised ellipsoid for the western segment is compatible with the ellipsoid that we propose for the eastern segment with a difference in strain orientation of ~30° angle. We discuss the possible reasons for this E-W rotation in the following. Thus, the overall N54° trending Anegada Passage, from the Whiting Basin to the Lesser Antilles forearc, is likely a 450 km long E-W trending en échelon left-lateral strike-slip tectonic system, with a main strike-slip strain rotating from a WNW-ESE direction to the east of the Anegada Canyon to a NW-SE direction to the west.

5.3. Polyphased Deformation Model

5.3.1. Past Deformation

In the Sombrero Basin, above the homogeneously thick unit SB, the northward dipping fan-shaped unit SC indicates that an extensive, possibly transtensive, tectonic phase opened a deep basin mostly controlled by the fault F2 (Figure 6). In the Malliwana Basin, unit MC, which overlies the homogeneously thick unit MB, drastically thickens at the basin axis, highlighting an abrupt extensive to transtensive tectonic phase (Figure 8). The E-W to WSW-ENE orientation of the basin axis associated with the northward dipping sedimentary fan suggest a N-S to NW-SE extension. This interpretation is consistent with previous tectonic models [*Jany et al*., 1990; *Mann et al*., 2005; *Raussen et al*., 2013] which conclude to similar extension along the western segment of the Anegada Passage. According to these authors, the Bahamas Bank docking against the Caribbean Plate along the Puerto Rico Trench during the Miocene triggered an ENEward escape [*Jany et al*., 1990] or an anticlockwise rotation of the PRVI block [*Masson and Scanlon*, 1991; *Mann et al*., 2005]. Based on previous work and our global new data set we propose that this tectonic phase generated the deep crustal E-W faulting along a paleo-system Anegada Passage, opening locally the Sombrero Basin and the Malliwana Basin.

5.3.2. Partitioning

Recent unit SD conformably and homogeneously blankets the Sombrero Basin as well as recent units in the Virgin Islands and the Whiting Basins [*Raussen et al*., 2013; *Chaytor and ten Brink*, 2015]. Thus, the N-S to NW-SE extension tended to decrease through times and is likely to be extinct nowadays. In contrast, F2 was recently reactivated in a strike slip to transpressive fault and the Malliwana Basins has undergone transpressive deformation. In the following, we discuss the possible relation between these recent strike-slip deformations and the strain partitioning in the frame of an oblique subduction zone.

Strike-slip faults systems in the overriding plate frequently accommodate the trench-parallel shear component [*McCaffrey*, 1992]. When they are neo-formed, these strike-slip faults are optimally oriented compared to the convergence vector [e.g., *Leever et al*., 2011; *Martinez et al*., 2002; *McClay et al*., 2004]. At early stages, the strike slip is first taken up along planes R oriented at a 30° angle to the shear direction and then progressively rotates, at later stages, up to a direction subparallel to the shear. However, in various oblique subduction zones, the shear component is accommodated along inherited faults with various orientations, not necessarily optimal, as for instance in Nankai system [*Tsuji et al*., 2014].

In the northern Lesser Antilles, offshore of Puerto Rico and Virgin Islands, the trench-parallel shear generated the left-lateral strike-slip Bunce Fault [*ten Brink et al*., 2004]. The new bathymetric map indicates that this fault extends to 17.5°N with a direction subparallel to the deformation front and thus to the shear strain component [*Marcaillou et al*., 2014]. This direction is thus consistent with the northern Lesser Antilles strain-partitioning tectonic system. In contrast, the E-W orientation of the left-lateral strike-slip faulting along the Anegada Passage appears to be poorly compatible with a mature neo-formed strike-slip system related to the WNW-ESE main shear strain. However, this E-W sinistral faulting correspond with planes R (Figure 9). Thus, we propose that the WNW-ESE shear strain due to the oblique convergence vector first reactivated, as planes R, E-W faults inherited from the previous extensive tectonic phase. The crustal depth and weakness of these inherited faults possibly prevent the strike-slip system from evolving at a later stage to a WNW-ESE direction that would have been more consistent with the global shear strain direction. As a result, new bathymetric and seismic data acquired during Antithesis 1 and 3 cruises reveal a polyphased tectonic history of the Anegada Passage that we summarize in the following discussion.

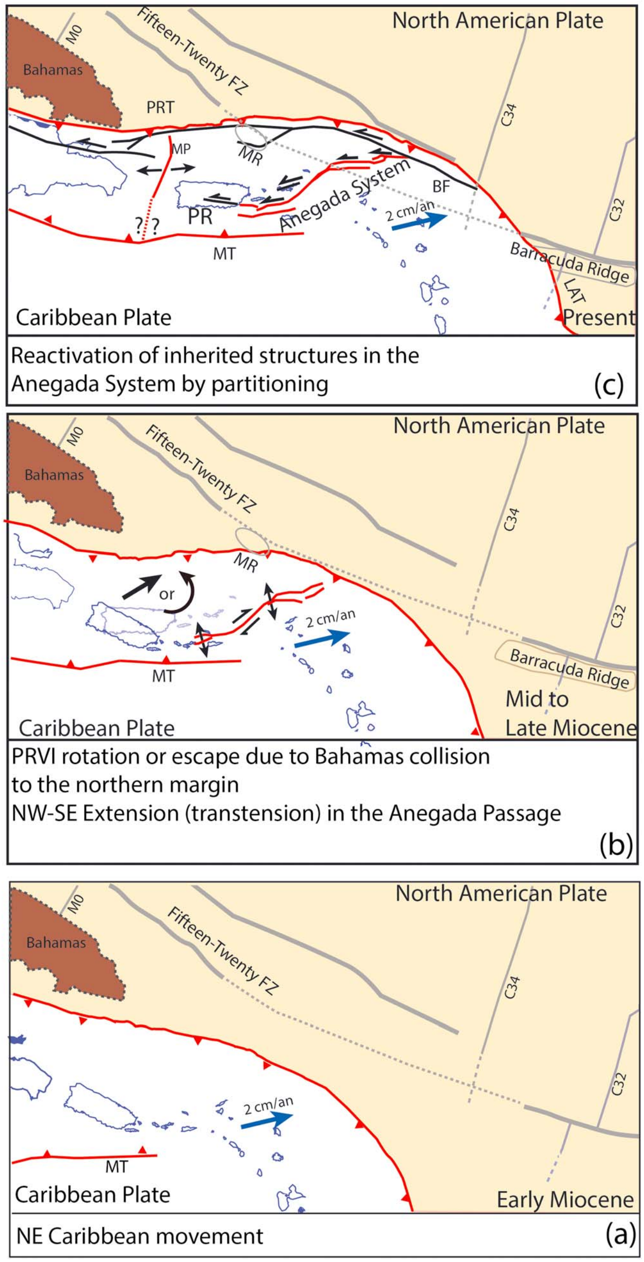

Figure 10. Interpretative reconstruction of PRVI regional kinematic from Lower Miocene modified from *Calais et al*. [2016]. Brown: Bahamas Carbonate Platform, Beige: North American Plate, Red lines: main faults, Thick grey lines: fracture zone; Thin grey lines: ridges, fault zone, and magnetic anomalies are from *Pichot* [2012]; Blue lines: Lesser and Greater Antilles Islands; Blue arrow: North American/Caribbean Plates motions; Black arrow: tectonic deformation; BF: Bunce Fault; LRT: Lesser Antilles Trench; PRT: Puerto Rico Trench; MP: Mona Passage; and MT: Muertos Through.

5.4. Geodynamic Model

We propose a three-step geodynamic evolution from early Miocene to present, by integrating our observations in the Lesser Antilles forearc to previously published models.

1. 20 Ma ago, prior to the collision of the Bahamas carbonate platform, the Caribbean Plate was moving northeastward [*Grindlay et al*., 2005], and the PRVI block and the Anegada Passage did not exist yet (Figure 10a).
2. The collision of the Bahamas Platform during the Mid to Late Miocene [e.g., *Grindlay et al*., 2005] against the Caribbean Plate in the Puerto Rico trench results in a ENEward escape [*Jany et al*., 1990] or anticlockwise rotation of the PRVI block [*Masson and Scanlon*, 1991; *Mann et al*., 2005]. This kinematic reorganization possibly triggered N-S to NW-SE extension and the resulting E-W to NE-SW normal faulting that structured the basins of the paleo-system Anegada Passage (Figure 10b).
3. This Paleo system has more recently been reactivated in a left-stepping sinistral strike-slip system likely related to a WNW-ESE sinistral strike-slip shear, compatible with the margin tectonic partitioning in the frame of the oblique subduction (Figure 10c).

Thus, this tectonic interpretation is consistent with the models of the ENEward escape [*Jany et al*., 1990] (Figure 4c) or the anticlockwise rotation of the PRVI block [*Masson and Scanlon*, 1991; *Mann et al*., 2005] (Figure 4d), but not with the left-lateral strike-slip model proposed by *Mann and Burke* [1984] (Figure 4b). This new geodynamic model also differs from the interpretation by *Feuillet et al*., 2002 who proposed that the strain partitioning causes active NW-SE extension in the Lesser Antilles forearc opening the NE-SW elongated basins. We do not rule out possible local tectonic extension in the area, but the data presented here highlight that this extensive tectonic phase climaxed in the past and has mostly been relayed by left-lateral strike-slip deformations. A unique unvarying geodynamic cause, the strain partitioning, would hardly be responsible for this drastic tectonic change. Along the western and eastern segments of the Anegada Passage, the main shear strain is interpreted to be WSW-ENE [*Raussen et al.*, 2013] and WNW-ESE (this study), respectively. Various geodynamic features vary from west to east and may interfere with the strain partitioning resulting in this 30° anticlockwise rotation. The western segment is possibly impacted by the proximity to the Muertos Through, the Greater Antilles strike-slip systems, or even the Bahamas Bank collision zone. Moreover, the westward increasing depth of the steep slab and the decreasing interplate coupling at great depth possibly reduce the control onto the back-arc tectonic pattern by the strain partitioning related to the oblique subduction zone.

The Antithesis data reveal recent partitioning deformation across the NE Anegada Passage. Nevertheless, actual observations deduced from GPS data [*Symithe et al.*, 2015; *Calais et al.*, 2016] suggest a small amount of slow deformation also supported by a low level of seismicity along the Anegada Passage. The small but nonzero deformation can be explained by the low subduction convergence and thus a very low trench-parallel shear component displacement shared out between the Bunce fault and the Anegada Passage.

6. Conclusion

This paper based on new seismic data and multibeam bathymetry proposes a reinterpretation of the structure and the tectonic pattern of the poorly investigated Anegada Passage.

In the northern Lesser Antilles forearc, the newly observed eastward segment of this passage is an E-W trending strike-slip system that consists in a set of active E-W strike-slip faults, pull-apart basins, and restraining bends. The overall structure of this segment indicates an active WNW-ESE sinistral strike-slip system and thus a NE-SW $\sigma 1$ compressive and a NW-SE $\sigma 3$ extensive axes.

This interpretation is globally consistent with the previously published [*Raussen et al.*, 2013] direction of the pull-apart basins axis and the main strike-slip faults within the western segment of the Anegada Passage. We thus conclude that the overall N54° trending Anegada Passage, from the Whiting Basin to the Lesser Antilles margin front, is a 450 km long en échelon left-lateral strike-slip tectonic system, with a main strike-slip strain rotating from a WNW-ESE direction to the east of the Anegada Canyon to a WSW-ENE direction to the west.

The deep sedimentary structure within the basins suggests that the Anegada Passage opening is related to a past NW-SE to N-S extensive tectonic phase. This interpretation is consistent with previous tectonic models which proposed that this extension resulted from the ENEward escape or the anticlockwise rotation of the PRVI block, as a consequence of the Bahamas Bank docking against the Caribbean Plate in the Puerto Rico trench during the Miocene. However, the current WNW-ESE shear strain taken up by the E-W sinistral strike-slip system is more likely to be related to the plate convergence obliquity and the margin strain partitioning.

Acknowledgments
We thank the Captain and the crew of the RVs *L'Atalante* and *Pourquoi Pas?* We are indebted to the Genavir Technicians for bathymetry processing, the successful completion of the seismic acquisition, and to the scientific crew for the preprocessing completed on board. We gratefully acknowledge financial support from Region Bretagne for the PhD fellowship of M. Laurencin, Labex MER and INSU, and Antilles University of Guadeloupe Island for the cruise. Multichannel processing has been done with Geocluster software of CGG and with Seismic Unix for the figures. Most of the figures were drafted using GMT, Qgis, and Adobe Illustrator software. Every geophysical data of the Antithesis cruises are available on demand at SISMER (www.ifremer.fr/sismer/).

References

Andrews, B., U. S. ten Brink, W. Danforth, J. D. Chaytor, J. L. Granja Bruña, P. Llanes Estrada, and A. Carbó-Gorosabel (2013), Bathymetric terrain model of the Puerto Rico trench and the northeastern Caribbean region for marine geological investigations. USGS Report: 19.

Armijo, R., N. Pondard, B. Meyer, G. Uc, S. Schmidt, and C. Rangin (2005), Submarine fault scarps in the sea of Marmara pull-apart (North Anatolian Fault): Implications for seismic hazard in Istanbul, *Geochem. Geophys. Geosyst.*, *6*, Q06009, doi:10.1029/2004GC000896.

Barnes, P. M., R. Sutherland, B. Davy, and J. Delteil (2001), Rapid creation and destruction of sedimentary basins on mature strike-slip faults: An example from the offshore Alpine Fault, New Zealand, *J. Struct. Geol.*, *23*, 1727–1739.

Burg, J. P. (2013), Strike-slip and oblique-slip tectonics, *Struct. Geol. and Tectonics*, 157–176.

Byrne, D. B., G. Suarez, and W. R. Mccann (1985), Muertos trough subduction-microplate tectonics in the northern Caribbean, *Nature*, *317*, 420–421.

Calais, E., S. J. Symithe, B. Mercier De Lepinay, and C. Prépetit (2016), Plate boundary segmentation in the northeastern Caribbean from geodetic measurements and Neogene geological observations, *C. R. Geosci.*, *348*, 42–51, doi:10.1016/j.crte.2015.10.007.

Chaytor, J. D., and U. S. ten Brink (2015), Event sedimentation in low-latitude deep-water carbonate basins, Anegada Passage, northeast Caribbean, *Basin Res.*, *27*, 310–335, doi:10.1111/bre.12076.

Christie-Blick, N., and K. Biddle (1985), Deformation and basin formation along strike-slip faults. Strike-slip deformation, basin formation and sedimentation, *SEPM Spec. Publ.*, *37*, 1–34, doi:10.2110/pec.85.37.0001.

Corbeau, J., F. Rolandone, S. Leroy, B. Mercier De Lepinay, B. Meyer, N. Ellouz-zimmermann, and R. Momplaisir (2016), The northern Caribbean plate boundary in the Jamaica Passage: Structure and seismic stratigraphy, *Tectonophysics*, *675*, 209–226, doi:10.1016/j.tecto.2016.03.022.

DeMets, C., P. Jansma, G. Mattioli, T. H. Dixon, F. Farina, R. Bilham, E. Calais, and Mann (2000), GPS geodetic constraints on Caribbean-North America plate motion, *Geophys. Res. Lett.*, *27*, 437–440, doi:10.1029/1999GL005436.

Feuillet, N., Manighetti, I., Tapponnier, P., and Jacques, E. (2002), Arc parallel extension and localization of volcanic complexes in Guadeloupe, Lesser Antilles, *J. Geophys. Res. 107*(B12), 2331, doi:10.1029/2001JB000308.

Fossen, H. (2010) Chapter 18 : Strike-slip, transpression and transtension, in *Structural Geology*, pp. 355–370, Cambridge Univ. Press.

Garfunkel, Z., and Z. Ben-Avraham (1996), The structure of the Dead Sea basin, *Tectonophysics*, *266*, 155–176.

Grindlay, N. R., P. Mann, J. F. Dolan, and J. P. Van Gestel (2005), Neotectonics and subsidence of the northern Puerto Rico-Virgin Islands margin in response to the oblique subduction of high-standing ridges, in *Active Tectonics and Seismic Hazards of Puerto Rico, the Virgin Islands, and Offshore Areas*, *Geol. Soc. Am. Spec. Pap.*, *385*, edited by P. Mann and C. Prentice, pp. 31–60.

Harding, T. P. (1976), Tectonic significance and hydrocarbon trapping consequences of sequential folding synchronous with San Andreas faulting, San Joaquin Valley, California, *Am. Assoc. Pet. Geol. Bull.*, *60*, 356–378.

Holcombe, T. (1978), Geomorphology and subsurface geology West of Saint Croix. U.S. Virgin Islands, in *Geological and Geophysical Investigations of Continental Margins*, edited by J. S. Watkins, L. Montadert, and P. W. Dickerson, pp. 353–362, Am. Assoc. Petrol. Geol. Mem.

Jansma, P. E., G. S. Mattioli, A. M. López, C. DeMets, T. H. Dixon, P. Mann, and E. Calais (2000), Neotectonics of Puerto Rico and the Virgin Islands, northeastern Caribbean, from GPS geodesy, *Tectonics*, *19*, 1021–1037, doi:10.1029/1999TC001170.

Jany, I., K. M. Scanlon, and A. Mauffret (1990), Geological interpretation of combined Seabeam, Gloria and seismic data from Anegada Passage (Virgin Islands, North Caribbean), *Mar. Geophys. Res.*, *12*, 173–196, doi:10.1007/BF02266712.

Laurencin, M., D. Graindorge, B. Marcaillou, F. Klingelhoefer, M. Evain, and J. F. Lebrun (2015), Is the Anegada Passage a sealed structure related to a past tectonic phase? A tectono-structure study of the Northern Lesser Antilles margin based on the Antithesis-1 cruise geophysical data Geodynamic context structure related to a past tectonic phase? Poster AGU.

Leever, K. A., R. H. Gabrielsen, J. I. Faleide, and A. Braathen (2011), A transpressional origin for the West Spitsbergen fold-and-thrust belt: Insight from analog modeling, *Tectonics*, *30*, TC2014, doi:10.1029/2010TC002753.

Leroy, S., et al. (2015), Segmentation and kinematics of the North America-Caribbean plate boundary offshore Hispaniola, *Terra Nova*, *27*, 467–478, doi:10.1111/ter.12181.

Leroy, S., A. Mau, P. Patriat, and B. Mercier De Lepinay (2000), An alternative interpretation of the Cayman trough evolution from a reidentification of magnetic anomalies, *Geophys. J. Int.*, *141*, 539–557.

Mann, P., and K. Burke (1984), Neotectonics of the Caribbean, *Rev. Geophys.*, *22*, 309–362, doi:10.1029/RG022i004p00309.

Mann, P., J.-C. Hippolyte, N. R. Grindlay, and L. J. Abrams (2005), Neotectonics of southern Puerto Rico and its offshore margin, *Geol. Soc. Am. Spec. Pap.*, *385*, 173–214, doi:10.1130/0-8137-2385-X.173.

Mann, P., F. W. Taylor, R. L. Edwards, and T. Ku (1995), Actively evolving microplate formation by oblique collision and sideways motion along strike-slip faults: An example from the northeastern Caribbean plate margin, *Tectonophysics*, *246*, 1–69, doi:10.1016/0040-1951(94)00268-E.

Marcaillou, B., and Klingelhoefer, F. (2013), ANTITHESIS-1-Leg1 Cruise, RV L'Atalante. Cruises *Report*. doi:10.17600/13010070.

Marcaillou, B., et al. (2014), Les petites Antilles du Nord, une zone de subduction à faible couplage interplaque? Un nouvel éclairage tectono-structural et thermique fourni par la campagne ANTITHESIS. Poster Réunion des Sciences de la Terre.

Martinez, A., J. Malavielle, S. Lallemand, and J. Y. Collot (2002), Partition de la déformation dans un prisme d'accrétion sédimentaire en convergence oblique: Approche expérimentale, *Bull. Soc. Geol. Fr.*, *173*, 17–24, doi:10.2113/173.1.17.

Masson, D. G., and K. M. Scanlon (1991), The neotectonic setting of Puerto Rico, *Geol. Soc. Am. Bull.*, *103*, 144–154, doi:10.1130/0016-7606(1991)103<0144:TNSOPR>2.3.CO;2.

McCaffrey, R. (1992), Oblique plate convergence, slip vectors, and forearc deformation, *J. Geophys. Res.*, *97*(B6), 8905–8915, doi:10.1029/92JB00483.

McClay, K., and M. Bonora (2001), Analog models of restraining stepovers in strike-slip faults systems, *Am. Assoc. Pet. Geol. Bull.*, *2*, 233–260.

McClay, K., and T. Dooley (1995), Analogue models of pull-apart basins, *Geology*, *23*, 711–714.

McClay, K. R., P. S. Whitehouse, T. Dooley, and M. Richards (2004), 3D evolution of fold and thrust belts formed by oblique convergence, *Mar. Pet. Geol.*, *21*, 857–877, doi:10.1016/j.marpetgeo.2004.03.009.

Pichot, T. (2012), Les rides de Barracuda et de Tiburon, à l'est de la subduction des Petites Antilles: Origine, évolution et conséquences. Thesis Université de Brest Occidentale: 286.

Raussen, S., H. Lykke-Andersen, and A. Kuijpers (2013), Tectonics of the Virgin Islands Basin, north eastern Caribbean, *Terra Nova*, *25*, 252–257, doi:10.1111/ter.12033.

Reid, J., P. Plumley, and J. Schellekens (1991), Paleomagnetic evidence for late Miocene counterclockwise rotation of north coast carbonate sequence, Puerto Rico, *Geophys. Res. Lett.*, *18*, 565–568, doi:10.1029/91GL00401.

Smith, W. H. F., and D. T. Sandwell (1997), Global sea floor topography from satellite altimetry and ship depth soundings, *Science*, *277*, 1956–1962.

Speed, R. C., and D. K. Larue (1991), Extension and transtension in the plate boundary zone of the northeastern Caribbean, *Geophys. Res. Lett.*, *18*, 573–576.

Sylvester, A. (1988), Strike-slip faults, *Geol. Soc. Am. Bull.*, *100*, 1666–1703.

Sylvester, A., and R. Smith (1976), Tectonic transpression and basement-controlled deformation in San Andreas fault zone, Salton trough, California, *Am. Assoc. Pet. Geol. Bull.*, *60*, 2081–2102.

Symithe, S., E. Calais, J. B. de Chabalier, R. Robertson, and M. Higgins (2015), Current block motions and strain accumulation on active faults in the Caribbean, *J. Geophys. Res. Solid Earth*, *120*, 3748–3774, doi:10.1002/2014JB011779.

ten Brink, U., W. Danforth, C. Polloni, B. Andrews, P. Llanes, S. Smith, E. Parker, and T. Uozumi (2004), New seafloor map of the Puerto Rico trench helps assess earthquake and tsunami hazards, *Eos Trans. AGU*, *85*, 349–360, doi:10.1029/2004EO370001.

Tsuji, T., J. Ashi, and Y. Ikeda (2014), Strike-slip motion of a mega-splay fault system in the Nankai oblique subduction zone, *Earth Planets Space*, *66*, 1–14.

Van Benthem, S., R. Govers, and R. Wortel (2014), What drives microplate motion and deformation in the northeastern Caribbean plate boundary region?, *Tectonics*, *33*, 850–873, doi:10.1002/2013TC003402.

Vila, J. M., P. Andreieff, H. Bellon, and A. Mascle (1986), Tectonique de collage le long d' un accident décrochant, ante oligocène, est-ouest, dans les Iles Vierges septentrionales (Antilles) = Collage along an East-West transcurrent fault of ante-Oligocene age in the Northern Virgin Islands (West Indies), *C. R. Acad. Sci., Ser. IIa: Sci. Terre Planets*, *302*, 141–144.

Wu, J., K. Mcclay, P. Whitehouse, and T. Dooley (2009), 4D analogue modelling of transtensional pull-apart basins, *Mar. Pet. Geol.*, *26*, 1608–1623, doi:10.1016/j.marpetgeo.2008.06.007.